



## Effect of $\text{Mg}^{2+}$ , $\text{Li}^+$ , $\text{Na}^+$ and $\text{K}^+$ on the electrocrystallization of nickel from aqueous sulfate solutions containing boric acid

B.C. TRIPATHY<sup>1</sup>, S.C. DAS<sup>2</sup>, P. SINGH<sup>1\*</sup>, G.T. HEFTER<sup>1</sup> and D.M. MUIR<sup>3</sup>

<sup>1</sup>Department of Chemistry, Murdoch University, South Street, Murdoch, WA 6150, Australia

<sup>2</sup>Regional Research Laboratory (CSIR), Bhubaneswar 751013, Orissa, India

<sup>3</sup>Division of Minerals, CSIRO, PO Box 90, Bentley, WA 6102, Australia

(\*author for correspondence)

Received 21 December 1999; accepted in revised form 28 November 2000

**Key words:** boric acid, current efficiency, electrocrystallization, exchange current density, magnesium, nickel, nucleation overpotential

### Abstract

The effects of metal ions such as  $\text{Mg}^{2+}$ ,  $\text{Li}^+$ ,  $\text{Na}^+$  and  $\text{K}^+$  on the cathodic current efficiency, deposit morphology, crystallographic orientation and polarization behaviour during nickel deposition on stainless steel from aqueous sulfate solutions containing boric acid were investigated. There was virtually no change in current efficiency in presence of these metal ions, but changes were observed in the deposit morphologies and crystal orientations even though all the deposits looked bright, smooth and coherent. Changes were also observed in the polarization behaviour during nickel electrocrystallization in presence and absence of boric acid. An attempt has been made to correlate the effect of these metal ions on various parameters studied.

### 1. Introduction

Nickel electrodeposition is sensitive to the presence of metallic impurities particularly Cr, Al, Mg, Fe, Cu and Zn [1, 2]. Gogia and Das [2], who studied the effect of  $\text{Mg}^{2+}$ ,  $\text{Mn}^{2+}$ ,  $\text{Al}^{3+}$  and  $\text{Zn}^{2+}$  during nickel electrodeposition, found that while there was no significant effect on current efficiency (CE) at very low concentrations, the deposit characteristics and polarization behaviour are affected strongly. In a separate study [3], they reported that  $\text{Co}^{2+}$ ,  $\text{Cu}^{2+}$ ,  $\text{Fe}^{2+}$  and  $\text{Fe}^{3+}$  also have similar effect on nickel electrowinning at low concentration. But higher concentration levels (e.g.,  $1000 \text{ mg dm}^{-3} \text{ Co}^{2+}$  and  $250 \text{ mg dm}^{-3} \text{ Cu}^{2+}$ ) produced cracked, peeled and black nodular deposits.

The effect of  $\text{Mg}^{2+}$  on the electrowinning of nickel is of particular interest to the mining industry because relatively high concentrations of  $\text{Mg}^{2+}$  tend to remain in the hydrometallurgical leach liquor even after the solvent extraction step. The presence of  $\text{Mg}^{2+}$  has been reported to be both beneficial [4–14] and harmful [15–17]. Further work in this direction is highly desirable. Likewise depending on the nature of the ore body, alkali metal ions such as  $\text{Li}^+$ ,  $\text{Na}^+$  and  $\text{K}^+$  also are found in the hydrometallurgical liquors from which nickel metal is electrowon. However, there are hardly any reports on the effects of these metal ions on the electrochemical characteristics and morphology of the nickel deposits. Nor has the polarization behaviour

during nickel electrocrystallization in the presence of these metal ions been investigated in detail.

The role of boric acid during nickel electrodeposition is also not clearly understood. It has been reported that boric acid serves as a pH buffer [18], complexing agent [19] and catalyst [18, 20, 21] for nickel electrodeposition.

The purpose of the present investigation is to evaluate the effect of  $\text{Mg}^{2+}$  and the alkali metal ions on the electrodeposition characteristics of nickel from aqueous sulfate medium in terms of CE, deposit morphology, crystal orientations at  $60^\circ\text{C}$  the temperature at which nickel is usually electrowon in the mineral industry. The effect of  $\text{Mg}^{2+}$ ,  $\text{Li}^+$ ,  $\text{Na}^+$  and  $\text{K}^+$  on the kinetics and nucleation of nickel on stainless steel electrode was investigated by carrying out polarization measurements at  $25^\circ\text{C}$ .

### 2. Experimental details

#### 2.1. Rectangular flow cell

Nickel electrodeposition was carried out in a rectangular flow-through cell of dimension  $13.2 \text{ cm} \times 8 \text{ cm} \times 6 \text{ cm}$  made from perspex, consisting of separate cathodic and anodic compartments each of dimensions  $9 \text{ cm} \times 4 \text{ cm} \times 2 \text{ cm}$  separated by a microporous Daramic separator. Cathode and anode, each of area  $20 \text{ cm}^2$ ,

were fitted to the respective compartments. Then the two halves with the separator in between were clamped together using viton O-rings. The anolyte and catholyte were circulated in to their respective compartments by separate peristaltic pumps (Cole-Parmer Instrument company, Australia, model 7553-75) through inlet and outlet ports made from teflon. One extra port was provided to each compartment to admit a reference electrode for measuring cathode and anode potentials.

## 2.2. Reagents

For preparing electrolytes for different experiments ultrapure water [Millipore MilliQ System] was used along with the following analytical grade chemicals: nickel sulfate ( $\text{NiSO}_4 \cdot 6 \text{H}_2\text{O}$ ), sodium sulfate ( $\text{Na}_2\text{SO}_4$ ), potassium sulfate ( $\text{K}_2\text{SO}_4$ ), magnesium sulfate ( $\text{MgSO}_4 \cdot 7 \text{H}_2\text{O}$ ), boric acid ( $\text{H}_3\text{BO}_3$ ), sulfuric acid ( $\text{H}_2\text{SO}_4$ ) all are from Univar, APS Finechem and lithium sulfate ( $\text{Li}_2\text{SO}_4 \cdot \text{H}_2\text{O}$ ) from BDH.

## 2.3. Electrode preparation

For the electrodeposition and polarization studies the surface of the electrode prior to metal electrodeposition was polished with 400 and then 1200 grade silicon carbide paper to mirror finish and then rinsed with 1 M HCl followed by ultra-pure water.

## 2.4. Electrolysis

All the electrodeposition experiments were conducted for two hours at a current density of  $200 \text{ A m}^{-2}$  by applying current from a regulated power supplier (0–30 V, 5 A, d.c. power supply, Dicksmith Electronics, China), precision voltmeter and ammeter were placed in the cell circuit to record the potentials and current. The flow rate of the electrolyte was maintained at  $1.8 \text{ L h}^{-1}$ . A thermostat (Grant (Selbys), Australia) was used for maintaining the electrolyte temperature at  $60 \pm 1 \text{ }^\circ\text{C}$ . The pH of the electrolyte was kept at 2.5 by addition of dilute sulfuric acid. Stainless steel and lead-antimony (Sb, 1–5%) were used as cathode and anode, respectively. All the potentials were measured and are quoted against a saturated calomel electrode (SCE). After electrolysis, the cathode was removed from the cell, thoroughly washed with water and then dried. The cathodic current efficiency was calculated from the weight gained by the cathode following electrolysis.

## 2.5. Polarization measurements

All the experiments for studying the polarization behaviour were carried out with  $100 \text{ cm}^3$  electrolyte at ambient temperature ( $25 \pm 1 \text{ }^\circ\text{C}$ ). A stainless steel disc electrode of 3 mm diameter (austenitic grade 316), platinum wire of 0.5 mm diameter and saturated calomel electrode were used as working, auxiliary and reference electrodes, respectively. A PAR (model 273A)

potentiostat/galvanostat was used for scanning the potential from 0 to  $-950 \text{ mV}$  at a scan rate of  $10 \text{ mV s}^{-1}$ . High purity nitrogen was used to sparge out dissolved oxygen and to maintain an inert atmosphere throughout the polarization studies.

## 2.6. Deposit examination

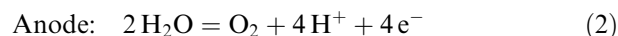
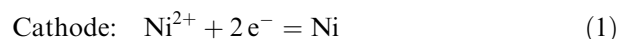
A Philips (PW 1050) X-ray diffractometer was used to examine the nickel deposits to determine their preferred crystal orientations. The surface morphology of the deposits was examined by scanning electron microscopy (SEM) using a Philips (XL 20 SE) microscope.

## 3. Results and discussion

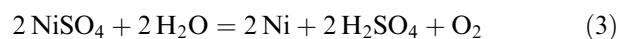
### 3.1. Cathodic current efficiency

Thermodynamically, the hydrogen evolution reaction is expected to interfere with the nickel electrodeposition process. Indeed nickel deposition from sulfate solutions is well known to be preceded by hydrogen evolution [20–25].

During nickel electrodeposition the main reactions, which occur at the electrodes are as follows:



With the overall cell reaction being



Thus, during electrolysis, the generation of  $\text{H}^+$  should cause a decrease in electrolyte pH. Therefore, to avoid the effect of changing pH on the nickel electrodeposition process, the electrolytic cell consisted of a cathode compartment separated from the anodic compartment by means of a microporous Daramic separator.

As noted in Table 1, the CE for nickel electrodeposited from pure nickel sulfate solution is 94%. The

Table 1. Effect of  $\text{Li}^+$ ,  $\text{Na}^+$ ,  $\text{K}^+$  and  $\text{Mg}^{2+}$  ions on nickel electrodeposition from nickel sulfate bath at pH 2.5 and  $60 \text{ }^\circ\text{C}$

Cation(s) added	Added cation concentration /M	Average cathode potential /V vs SCE	CE /%
Nil	Nil	-0.85	94
$\text{Mg}^{2+}$	0.063	-0.85	95
$\text{Mg}^{2+}$	0.63	-0.86	98
$\text{Li}^+$	0.168	-0.85	94
$\text{Na}^+$	0.168	-0.86	96
$\text{Na}^+$	1.68	-0.87	97
$\text{K}^+$	0.168	-0.85	96
$\text{Na}^+ + \text{Mg}^{2+}$	0.168 + 0.063	-0.86	98

( $\text{NiSO}_4 \equiv 1.022 \text{ M}$  and  $\text{H}_3\text{BO}_3 \equiv 0.194 \text{ M}$ )

influence of  $Mg^{2+}$  on the cathodic CE and average cathode potential is also given in the same table which also includes the results for  $Li^+$ ,  $Na^+$  and  $K^+$ . The data in Table 1 also show that irrespective of the cations present the cathodic current efficiency is virtually the same. The CE is almost constant at about 95%, independent of the identity of the cations investigated. At very high concentrations of  $Mg^{2+}$ , a slight increase (2–3%) in CE is seen.  $Na^+$  seems to parallel  $Mg^{2+}$  at higher concentration. The average cathode potential in the presence of all the investigated ions is around  $-0.85$  V and all the deposits look bright, smooth and coherent to the naked eye.

### 3.2. Crystallographic orientations

The X-ray analysis results of the electrodeposited nickel in the presence of the various metal ions are presented in Table 2. Both in pure nickel sulfate solution and in the presence of  $Li^+$  and  $K^+$  the order of the preferred orientation of the nickel deposit is (200) > (111). In the presence of  $Na^+$  the preferred orientation is the same as that for  $Li^+$  and  $K^+$  except that the intensity of the (111) peak is increased fourfold. Interestingly, the presence of  $Mg^{2+}$  results in a dramatically different XRD spectrum, which shows two additional peaks (311) and (220) with (311) as the strongest peak. Thus in the presence of  $Mg^{2+}$  the preferred orientation is (311) > (200) > (220) > (111).

Higher concentration of  $Mg^{2+}$  (0.63 M) did not alter the preferred orientation but increased the intensity of all the three peaks except that of the strongest (311) peak as compared to  $Mg^{2+}$  at lower concentration (0.063 M). A high concentration of  $Na^+$  (1.68 M) resulted in two additional peaks in the XRD spectrum but the (200) peak remained the strongest and the order of the preferred crystal orientation was (200) > (111) > (311) > (220). When both  $Na^+$  and  $Mg^{2+}$  were present together, the nickel deposit exhibited similar preferred orientation as that of  $Na^+$ , showing the effect of  $Na^+$  dominating over  $Mg^{2+}$ .

Table 2. Effect of  $Li^+$ ,  $Na^+$ ,  $K^+$  and  $Mg^{2+}$  ions on crystallographic orientations of nickel electrodeposits from sulfate baths at pH 2.5 and 60 °C

Cation(s) added	Added cation concentration /M	Crystal planes ( <i>h k l</i> ) Relative peak intensity ( $I_0/I$ )			
		(1 1 1)	(2 0 0)	(2 2 0)	(3 1 1)
Nil	Nil	36	100	–	–
$Mg^{2+}$	0.063	35	55	55	100
$Mg^{2+}$	0.63	68	84	50	100
$Li^+$	0.168	11	100	–	–
$Na^+$	0.168	62	100	–	–
$Na^+$	1.68	41	100	25	26
$K^+$	0.168	15	100	–	–
$Na^+ + Mg^{2+}$	0.168 + 0.063	84	100	–	8

( $NiSO_4 \equiv 1.022$  M and  $H_3BO_3 \equiv 0.194$  M)

Thus it is found that  $Li^+$ ,  $Na^+$  and  $K^+$  favoured the growth of the (200) plane as the most preferred as compared to  $Mg^{2+}$  which favours the growth of (311) plane. In the presence of both  $Na^+$  and  $Mg^{2+}$  together at low concentrations ( $Na \equiv 0.168$  M,  $Mg \equiv 0.063$  M) the effect of  $Na^+$  dominates favouring growth of the (200) plane.

### 3.3. Surface morphology

To the naked eye, the nickel electrodeposit obtained from pure nickel sulfate solution looked bright, smooth and coherent but those obtained from the sulfate solutions containing boric acid and metal ions such as  $Mg^{2+}$ ,  $Li^+$ ,  $Na^+$  and  $K^+$  looked brighter, smooth and coherent. However, a close examination of the morphology by SEM shows that the deposit characteristics are different in the presence of the different metal ions in the nickel electrolyte. It can be seen (Figure 1) that the nickel deposit obtained from pure nickel sulfate consists of round edged grains of varying sizes from 2–15  $\mu$ m. Larger crystals surrounded by small crystallites distributed nonuniformly can be seen throughout the deposit. Addition of  $Li^+$  to the above solution containing boric acid produced brighter, smooth and coherent deposits with sharp edged and randomly arranged crystals giving a compact deposit. Similar deposits are also observed with  $Na^+$ ,  $K^+$  and  $Mg^{2+}$  (Figure 2), although the size of the crystals was smaller than in the presence of  $Li^+$ . The nickel deposits from solutions containing  $Na^+$  and  $Mg^{2+}$  have more rounded crystal edges than those obtained from solutions containing  $Li^+$ . Random growth of the crystallites is seen in all the nickel deposits obtained in presence of the metal ions studied here. In the presence of high concentrations of  $Na^+$  or  $Mg^{2+}$  or their mixture at lower concentrations, the shape of the crystallites looked relatively more sharp edged.

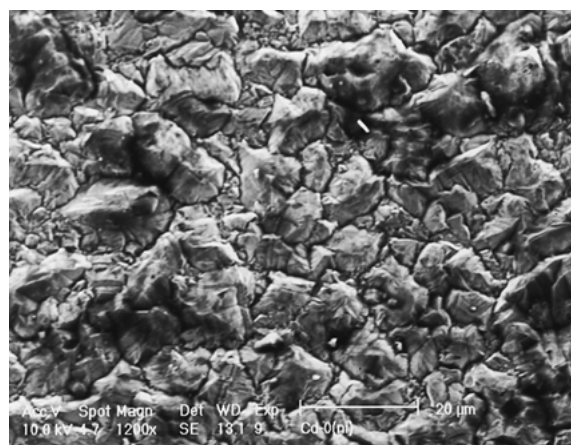


Fig. 1. SE micrograph showing the surface morphology of the nickel deposit obtained from pure  $NiSO_4$  solution.

## 3.4. Polarization studies

Figure 3 shows the polarization behaviour of nickel electrodeposition from pure nickel sulfate solution on a stainless steel electrode in the presence and absence of boric acid. It is evident that the electrodeposition of nickel is preceded by hydrogen evolution marked as 'A' in the Figure 3. Thus the  $i/V$  profile for nickel electrodeposition includes the  $H^+$  reduction current. Clearly boric acid influences the nickel deposition potential and polarizes it to more negative values. The nucleation potential ( $E_n$ ) which is defined as the intersection point on the x axis when the ascending portion of the cathodic scan is extrapolated. The  $E_n$  in the presence of boric acid is  $-905$  mV as compared to  $-880$  mV in its absence. The cross over potential ( $E_{co}$ ) which represents the point of

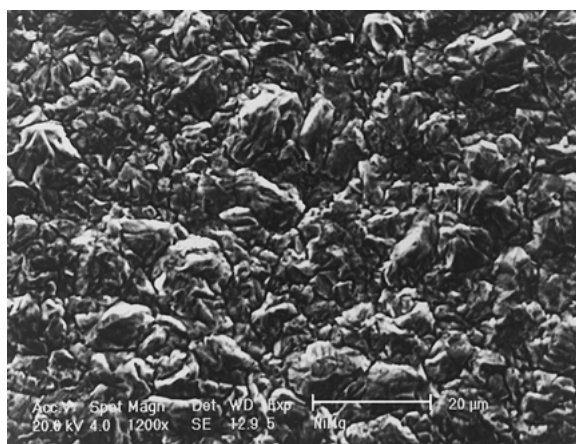


Fig. 2. SE micrograph showing the effect of  $Mg^{2+}$  (0.063 M) on the surface morphology of the nickel deposit.

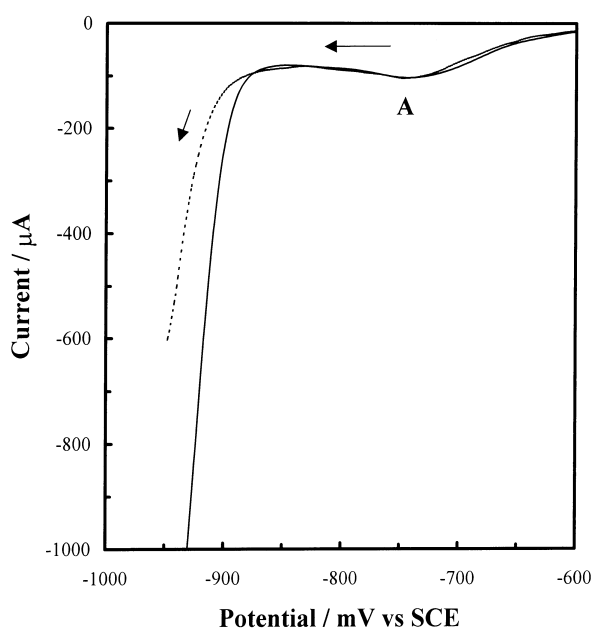


Fig. 3. Cathodic polarization of nickel electrodeposition from sulfate solution at pH 2.5. Key: (1)  $NiSO_4$  solution (1.022 M) (—); (2) [1] + boric acid (0.194 M) (- - - - -).

Table 3. Effect of  $Li^+$ ,  $Na^+$ ,  $K^+$  and  $Mg^{2+}$  ions on nucleation overpotential (NOP) and exchange current density ( $i_0$ ) for nickel electrodeposition from sulfate bath at pH 2.5 and  $25^\circ C$

Cation(s) added	Added cation concentration /M	NOP /mV		$i_0$ /mA cm <sup>-2</sup>	
		A*	B*	A*	B*
Nil	Nil	-160	-185	$2.0 \times 10^{-3}$	$2.2 \times 10^{-4}$
$Mg^{2+}$	0.063	-160	-186	$2.5 \times 10^{-3}$	$4.5 \times 10^{-4}$
$Mg^{2+}$	0.63	-163	-176	$1.4 \times 10^{-3}$	$4.1 \times 10^{-4}$
$Li^+$	0.168	-163	-176	$2.5 \times 10^{-3}$	$1.2 \times 10^{-3}$
$Na^+$	0.168	-168	-178	$1.1 \times 10^{-3}$	$6.3 \times 10^{-4}$
$Na^+$	1.68	-180	-195	$8.0 \times 10^{-4}$	$2.5 \times 10^{-4}$
$K^+$	0.168	-162	-190	$3.9 \times 10^{-3}$	$3.2 \times 10^{-4}$
$Na^+ + Mg^{2+}$	0.168 + 0.063	-165	-188	$1.5 \times 10^{-3}$	$6.1 \times 10^{-4}$

\* A = in absence of  $H_3BO_3$ , B = in presence of  $H_3BO_3$   
( $NiSO_4 \equiv 1.022$  M and  $H_3BO_3 \equiv 0.194$  M)

zero current during the reverse scan is  $-720$  mV for both the solutions.  $E_{co}$  represents the equilibrium potential of nickel (electrodeposited on the substrate) in contact with  $Ni^{2+}$  ions. Since boric acid in this case does not affect the equilibrium, the  $E_{co}$  value is the same in both the solutions. Of course, the  $E_n$  values are different because the adsorption of boric acid influences the electron transfer process at the electrode surface.

The nucleation overpotential (NOP) values ( $E_n - E_{co}$ ) and the exchange current density ( $i_0$ ) values as calculated from the polarization curves are given in Table 3. The NOP value for nickel electrodeposition from pure nickel sulfate solution is  $-160$  mV and that in the presence of boric acid is  $-185$  mV. Specific adsorption of boric acid on substrate is well known to slow down electron transfer reaction [24], which is also reflected in the lower

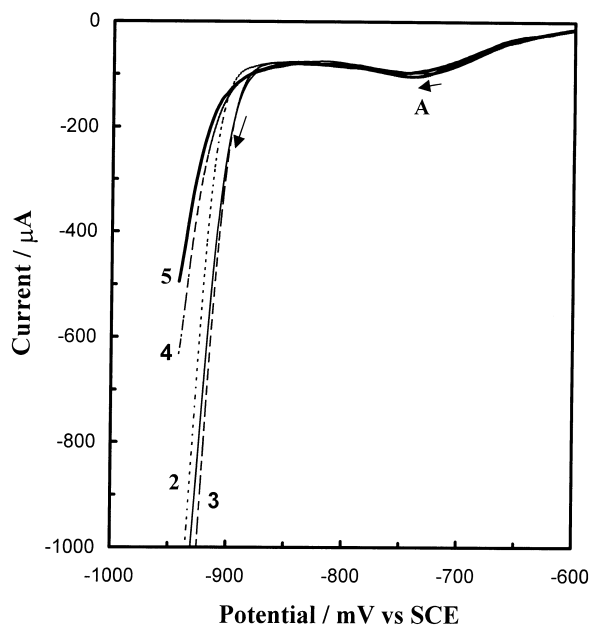


Fig. 4. Cyclic voltammograms of nickel sulfate solution at pH 2.5. Key: (1)  $NiSO_4$  solution (1.022 M) (—); (2) [1] +  $Na_2SO_4$  (0.168 M) (- - - - -); (3) [1] +  $MgSO_4$  (0.063 M) (- - - - -); (4) [2] + boric acid (0.194 M) (- · · · · -); (5) [3] + boric acid (0.194 M) (—).

exchange current density value (Table 3). The different  $i_0$  values indicate that the electron transfer process is affected by the presence of these metal ions, which may be attributed to their different adsorption behaviour.

The effect of all the investigated ions on the polarization of the cathode during nickel electrodeposition is found to be almost similar. Figure 4 is a typical example, which shows the effects of  $\text{Mg}^{2+}$  and  $\text{Na}^+$  in the presence and absence of boric acid. As can also be seen from the Table 3, in the absence and presence of boric acid the addition of  $\text{Mg}^{2+}$  up to 0.63 M has virtually no effect on the NOP of the electrodeposition of nickel which occurs at  $-880 \pm 3$  mV corresponding to the NOP value being  $-160 \pm 3$  mV. The addition of  $\text{Na}^+$  ions distinctly shifts the NOP value to slightly more negative potential. Thus, the NOP value at 0.168 M  $\text{Na}^+$  is  $-168 \pm 3$  mV and at 1.68 M the NOP is  $-180 \pm 3$  mV. Increase in NOP values correspond to decrease in  $i_0$  values indicating higher degree of adsorption and hence affecting the electron transfer process to more extent.

An interesting observation is that when  $\text{Mg}^{2+}$  is present together with  $\text{Na}^+$ , the effect of  $\text{Na}^+$  dominates the polarization behaviour which, as noted earlier, is also reflected in the exchange current density values (Table 3) and XRD data (Table 2).

In the presence of boric acid, the NOP value, as expected, is more negative than the corresponding value in its absence in all cases as also shown by lower  $i_0$  values. This indicates the formation of a stronger adsorption layer on the electrode surface.

#### 4. Conclusions

- (i) The presence of  $\text{Li}^+$ ,  $\text{Na}^+$ ,  $\text{K}^+$  and  $\text{Mg}^{2+}$  produces good nickel deposits from aqueous sulfate solutions containing boric acid producing bright, smooth and coherent deposit with high current yield.
- (ii) Combination of  $\text{Na}^+$  and  $\text{Mg}^{2+}$  at low concentrations shows similar deposition behaviour as that of  $\text{Na}^+$  only.
- (iii) Boric acid acts as brightener and cathodic polarizer.

#### Acknowledgements

Tripathy and Das thank R.P. Das and H.S. Ray for their encouragement. The authors also thank P. Fallon for assistance in SEM, K. Seymour for XRD and T.B. Issa for general assistance throughout the work. The financial support of the Australian Government under the Targeted Institutional Links Program and A.J. Parker Cooperative Research Centre for Hydrometallurgy is acknowledged.

#### References

1. B.C. Banerjee and A. Goswami, *J. Electrochem. Soc.* **106** (1959) 590.
2. S.K. Gogia and S.C. Das, *Metall. Trans. B* **19** (1988) 823.
3. S.K. Gogia and S.C. Das, *J. Appl. Electrochem.* **21** (1991) 64.
4. T.C. Eichstadt, *Metal Ind. (London)* **26** (1925) 603.
5. Anon, *Metallwaren-Ind.u. Galvano-Tech.* **23** (1925) 605.
6. S.M. Kochergein, *J. Appl. Chem. (USSR)* **12** (1939) 44.
7. S. Herrich, *Metal Ind. (NY)* **16** (1918) 1.
8. J. Underwood, *Monthly Rev. Am. Electroplaters' Soc.* **13** (1926) 14.
9. L.M. Evlannikov and D.S. Neiman, *Trans. Leningrad Ind. Inst., No. 1, Sec. Met. No. 1, 3* (1939).
10. H.J. Richards and F.P. Mennings, *Mon. Rev. Am. Electroplaters' Soc.* **12**(7) (1925) 23.
11. M.B. Diggin, *Mon. Rev. Am. Electroplaters' Soc.* **33** (1946) 513, 524.
12. J. Walters, *Mon. Rev. Am. Electroplaters' Soc.* **4** (1917) 10.
13. S. Makar'eva, *Bull. Acad. Sci. (USSR), Classe sci. math. nat., Ser. Chim.,* (1938), 1211 (in English) 1223.
14. D.W. Robinson, *Metal Ind. (NY)* **14** (1916) 133.
15. J. Haas, Jr., *Metal Ind. (NY)* **19** (1921) 364.
16. C.P. Madsen, *Trans. Am. Electrochem. Soc.* **39** (1921) 483.
17. R.E. Harr, *Trans. Electrochem. Soc.* **68** (1935) 425.
18. J. Ji, W.C. Cooper, D.B. Dreisinger and E. Peters, *J. Appl. Electrochem.* **25** (1995) 642.
19. B.V. Tilak, A.S. Gendron and M.A. Mosoiu, *J. Appl. Electrochem.* **7** (1977) 495.
20. J.P. Hoare, *J. Electrochem. Soc.* **134** (1987) 3102.
21. J.P. Hoare, *J. Electrochem. Soc.* **133** (1986) 2491.
22. R.K. Dorsch, *J. Electroanal. Chem.* **21** (1969) 495.
23. M. Fleischmann and A. Saraby-Reintjes, *Electrochim. Acta* **29** (1984) 69.
24. J. Horkans, *J. Electrochem. Soc.* **126** (1979) 1861.
25. M. Pushpavanam and K. Balakrishnan, *J. Appl. Electrochem.* **26** (1996) 283.